

Optimization of Anti-Impact Energy Absorption Structure of Hydraulic Support

Qiang ZHANG*, **, Baoqi LI***, Runxin ZHANG****

*Liaoning Technical University, Fuxin, China

**Shandong University of Science and Technology, Qingdao, China

***Liaoning Technical University, Fuxin, China

****Shandong University of Science and Technology, Qingdao, China, E-mail: 597418002@qq.com (Corresponding Author)

crossref <http://dx.doi.org/10.5755/j02.mech.32032>

1. Introduction

Coal dominates the energy ecosystem in China, and coal mines continue to be exploited on a large scale. However, coal mining is becoming increasingly difficult and the number of underground accidents has increased significantly [1, 2]. As the main provision for working face support, hydraulic supports are of great importance to the safety of underground mining. Rock blasts are major events, and typically have a great impact on the hydraulic bracket causing the hydraulic legs to bend and affecting its function. Therefore, it is important to develop impact-resistant hydraulic supports for safe mining at the working face [3-5].

To improve the safety of underground operation, some scholars have proposed an anti-impact energy absorption structure that can be used as hydraulic support. Based on the combination of dynamic analysis and static analysis, Pan [6-10] designed an energy absorbing member nested in the bottom side of the hydraulic support hydraulic leg, which reduced the impact damage to the support through the large deformation of the structure, Xu [11] analyzed their influence on the impact strength of the multilateral honeycomb structure from the perspective of unit size and relative density through the impact test. Xiong [12] studied the influence of the number and location of holes on the mechanical properties of honeycomb structures by combining experiment and simulation. Hou [13] studied the shear performance and compression performance of hexagonal honeycomb structures under quasi-static and impact states. Li [14] used FEM to analyze the influence of the stroke speed on the energy absorption of foam structure. Yungwrith [15] constructed a honeycomb-filled sandwich structure and analyzed the change process of impact energy through the ballistic test.

At present, most research on impact resistant hydraulic support focuses on roadway support, while less research has been done on working face support. In this paper, a honeycomb structure is proposed, and the dynamic model of a Single Hydraulic Support is constructed using FEM. The energy absorption effect of the honeycomb structure with different geometric parameters is studied, and the influence of each parameter on the energy absorption performance is analyzed to arrive at the final optimization scheme, which provides theoretical guidance for the working face support.

2. Anti-impact and energy-absorbing structure model of hydraulic support

The hydraulic support model is shown in Fig. 1, including the structure of the top plate, hydraulic legs, base and pins. In order to improve the calculation efficiency, the hydraulic support structure is simplified, and the hydraulic legs, main roof, and other supporting structures are retained.

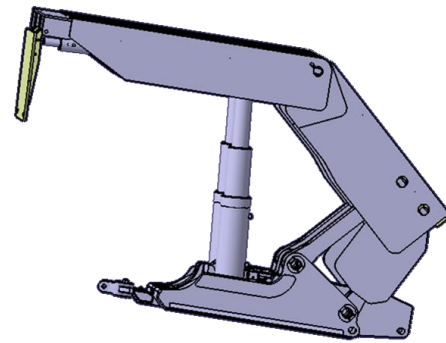


Fig. 1 Schematic diagram of hydraulic support structure

2.1. Simplified mechanical model of hydraulic support

The simplified hydraulic support model is shown in Fig. 2. Points *a* and *b* are the two ends of the roof, and point *c* is the joint between the hydraulic leg and roof, which is regarded as the particle point. f_1 is the resultant force on the hydraulic support of *ac* length, f_2 is the force on the simplified top beam model, f_3 is the resultant force on the hydraulic support of *db* section, where *ac* length $e_1 = 3064$ mm.

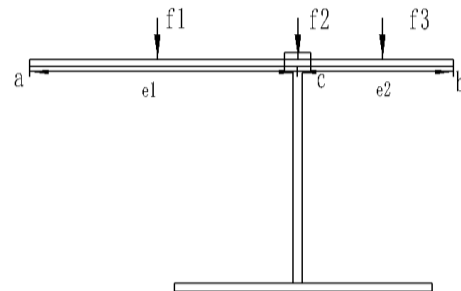


Fig. 2 Simplified mechanical model of hydraulic support

The length of section *db* is $e_2 = 1029$ mm, and the rated working resistance of the hydraulic support is the hydraulic leg supporting force of 10800 kN. Due to the support of the coal and rock mass, the stress on the top beam of the hydraulic support is regarded as equal load. According to

the proportional relationship, $f_1 = 7.16 f_2$, $f_3 = 2.07 f_2$, the force f_1 is equivalent to the force at point c , and the moment is calculated at point b , f_3 is equivalent to point c :

$$f_1 \times 2561 = f_{c1} \times 1029, \quad f_3 \times 3578.35 = f_{c3} \times 3064, \quad (1)$$

where: $f_{c1} = 2.489 f_1$, $f_{c3} = 1.13 f_3$.

Similarly, the force ratio of the simplified model in the width direction is 0.3531. Since the model has a single hydraulic leg, the rated working resistance of the simplified model is 90 kN. The hydraulic system of the hydraulic leg is modelled as a spring system, and the stroke of the hydraulic leg piston is 600 mm, so the spring stiffness is 150 N/mm.

2.2. Simplified mechanical model of hydraulic support

As shown in Fig. 3, the impact-resistant structure is the honeycomb sandwich structure inside the roof. As the height of the hydraulic support is limited, the height of the sandwich is set as 20 mm, where a and t represent the cell size and cell thickness, $a = 9$ mm, $t = 0.2$ mm, respectively.

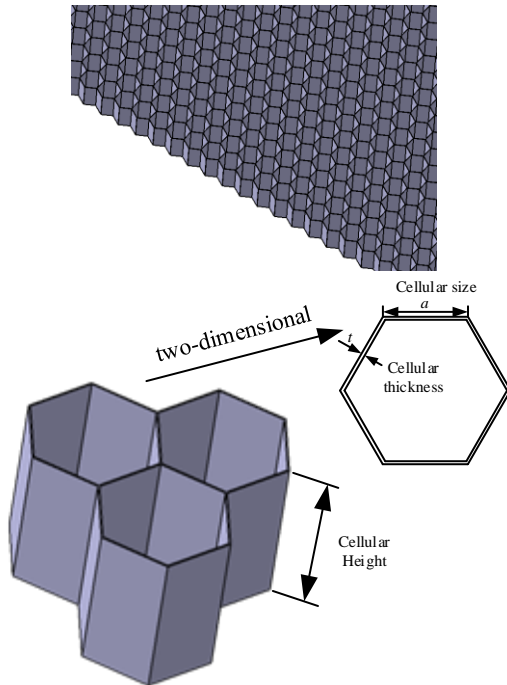
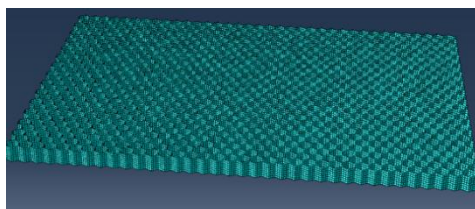
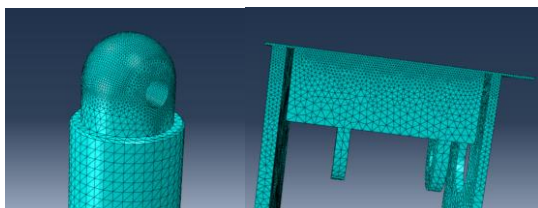


Fig. 3 Honeycomb structure model



Honeycomb structure



Hydraulic leg

Roof

Fig. 4 Meshing model of main components

The shell cell is used to divide the honeycomb structure, while the hexahedral cell is used to divide the roof, hydraulic legs, and other structures. The meshing model of the main components is shown in Fig. 4. Fixed constraints were added at the bottom of the column, and displacement constraints were added to the honeycomb structure to restrict other degrees of freedom except in the vertical direction.

3. Study of influence factors of energy absorption structure performance of hydraulic support

Taking the stress effect of the hydraulic leg and honeycomb structure as research indexes, the influence of structural parameters on the energy absorption effect of honeycomb structure was analyzed by the control variate method, taking cell size, cell thickness, and cell height as variables.

3.1. Effect of Cell size on anti-impact performance

The parameters of the cell structure are shown in Table 1. Since the cell thickness is much smaller than the other two dimensions, the shell unit is used to simulate the cell structure and divide a total of 770,776 elements, with an impact time of 0.05 s.

Table 1

Model parameter table with different cell size

Cell size	Cell thickness	Cell height	Impact velocity	Impact time
6 mm	0.2 mm	20 mm	200 mm/s	0.05 s
9 mm	0.2 mm	20 mm	200 mm/s	0.05 s
12 mm	0.2 mm	20 mm	200 mm/s	0.05 s

As the main supporting structure of the hydraulic support, the hydraulic leg is the main stress point. Therefore, the stress fields on the hydraulic leg in different cell models are extracted for comparison, and the stress of the hydraulic leg is mainly concentrated at the joint with the roof. When the cell size is 6 mm, 9 mm, and 12 mm, the force on the hydraulic leg is 136.1 MPa, 39.61 MPa and 60.74 MPa, respectively. In the model with the 9 mm cell size, the stress on the hydraulic leg decreases by 70% and 55%, respectively, compared with the model with 6 mm and 12 mm cell size. With the increase in cell size, the stress on the hydraulic leg decreases first and then increases.

To reflect the stress variation of the hydraulic leg during the whole impact process, the stress and displacement of the node at the connection between the hydraulic leg and roof are extracted as shown in Fig. 5.

The force on the hydraulic leg is small within 0–0.025 s, when the cell size is 6 mm, the hydraulic leg stress increases the fastest and the maximum is 142.6 MPa, which is much higher than the other two models. There is little difference in the collapse deformation before impact at 0.1s, and the displacement varies gradually after 0.1s. The deformation of the cell structure with 12 mm size is larger than that of the other two groups of models, and the maximum displacement is 16.23 mm.

The displacement of the roof and honeycomb structure are shown in Table 2; when the cell size increased, the hydraulic leg stress first decreased and then increased, and the displacement of the roof showed a decreasing trend, while that of the honeycomb structure showed an increasing

trend. Based on the calculation result, the honeycomb structure has the best impact resistance when the hole cell size is 9 mm.

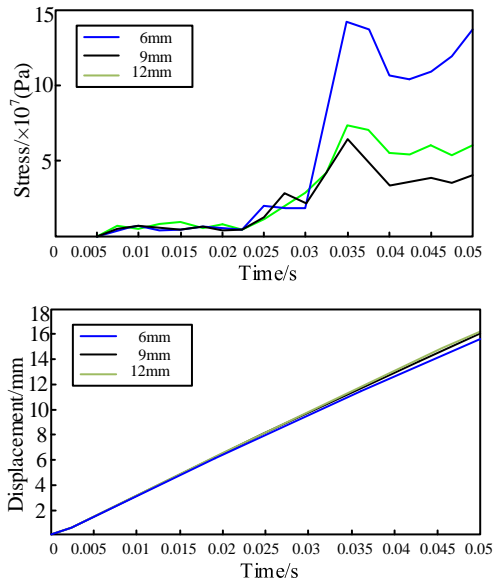


Fig. 5 Hydraulic leg stress and displacement curve

Table 2

Simulation results of different cell size models

Cell size	Hydraulic leg stress	Roof displacement	Honeycomb displacement
6 mm	142.6 MPa	0.5903 mm	15.53 mm
9 mm	64.54 MPa	0.4066 mm	16.03 mm
12 mm	73.20 MPa	0.3135 mm	16.23 mm

3.2. Effect of cell thickness on anti-impact performance

In this section, the effect of cell thickness on the impact resistance of the hydraulic support is studied for the honeycomb structure with a cell size of 9 mm and cell height of 20 mm. The cell thickness is 0.2, 0.4, and 0.6 mm, respectively. The boundary conditions are shown to Table 1.

When cell thickness is 0.2, 0.4, and 0.9 mm, the hydraulic leg stress is 39.61, 75.58 and 151 MPa, respectively. When the thickness of the cell is 0.2 mm, the stress on the hydraulic leg decreases 48% and 74%, respectively, compared with when the thickness of cell is 0.4 and 0.6 mm. With the increase in cell thickness, the stress on the hydraulic leg increases. The impact resistance of the honeycomb structure reduces with the increase in cell thickness. The stress and displacement of the node at the connection between the hydraulic leg and roof are extracted as shown in Fig. 6.

Within 0–0.025 s, the whole structure is in the elastic range, and the stress and displacement do not change much. It is worth noting that the hydraulic leg stress in the model of cell thickness of 0.2 mm is greater than the other two models, and the growth trend is much smaller than the others. After 0.01 s, the hydraulic leg stress shows an obvious growth for the 0.6 mm model with cell thickness, the growth trend of hydraulic leg stress is far greater than the other two models. This is mainly because the structural stiffness increases with the increase in thickness, and the honeycomb structure absorbs less energy. At this point, the roof displacement changes the most. Table 3 shows the displacement of the roof and honeycomb structure. In order to ensure

the maximum absorption energy of the honeycomb structure and reduce the stress on the hydraulic leg, the structure has the best impact resistance when the cell thickness is 0.2 mm.

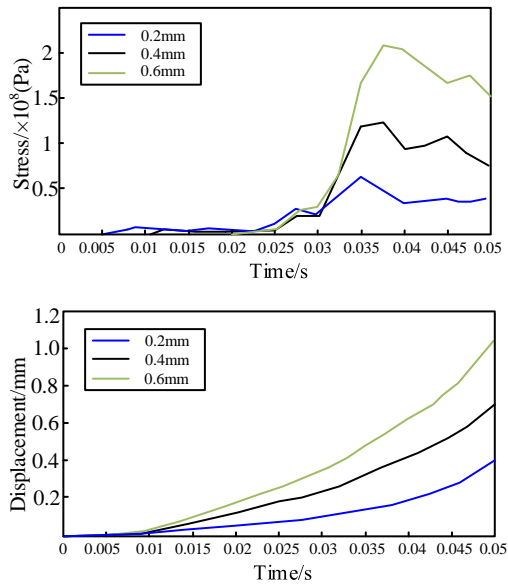


Fig. 6 Hydraulic leg stress and displacement curve

Table 3

Simulation results of different cell wall thickness models

Cell thickness	Hydraulic leg stress	Roof displacement	Honeycomb displacement
0.2 mm	64.54 MPa	0.4066 mm	16.03 mm
0.4 mm	122.8 MPa	0.7042 mm	15.13 mm
0.6 mm	207.3 MPa	1.046 mm	14.29 mm

3.3. Effect of cell height on anti-impact performance

This section studies the effect of cell height on the impact resistance of hydraulic support when cell size (9 mm) and thickness (0.2 mm) are constant. According to the actual supporting environment of the coal mine, the cell height is selected as 15 mm, 20 mm, and 25 mm. The boundary conditions are equivalent to Table 1.

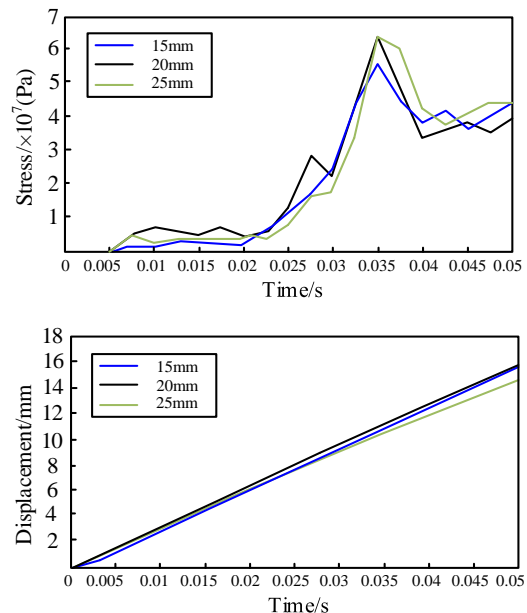


Fig. 7 Hydraulic leg stress and displacement curve

When cell height is 15, 20, and 25 mm, the stress on the hydraulic leg is 44.91, 39.61, and 44.51 MPa, respectively. In the model with cell height of 20 mm, the hydraulic leg stress is the least, which decreases by 11.8% and 10.9% when the cell height is 15 mm and 25 mm, respectively. Therefore, with the increase in cell height, the stress in the hydraulic leg decreases first and then increases.

The stress and displacement of the node at the connection between the hydraulic leg and roof are extracted as shown in Fig. 7.

In the three models, the stress on the hydraulic leg is small before 0.005 s, and then shows an increasing trend of varying degrees. After 0.025 s, the hydraulic leg stress of the three models increases gradually with the same value and reaches the maximum stress value at 0.035s. When the cell height is 20 mm, the deformation of the honeycomb structure is the largest (16.03 mm), and with the increase of cell height, the displacement of the honeycomb structure increased significantly and then decreased. Table.4 shows the displacement of the roof and honeycomb structure in the three models, and the honeycomb structure has better energy absorption effect when the cell height is 20 mm.

Table 4

Simulation results of different cell height models

Cell height	Hydraulic leg stress	Roof displacement	Honeycomb displacement
15 mm	56.64 MPa	1.602 mm	15.83 mm
20 mm	64.54 MPa	0.4066 mm	16.03 mm
25 mm	65.08 Mpa	0.4898 mm	14.73 mm

4. Research on energy absorption structure optimization of hydraulic support

4.1. Evaluation of energy absorbing structure performance

In order to reduce the damage to the hydraulic support by rock blast, the honeycomb structure should maximize the absorption of energy brought about by the rock blast, and the energy absorption characteristic is the direct criterion used to judge the performance of honeycomb structure. The absorption energy per unit mass is defined as:

$$SEA(d) = \frac{EA(d)}{M}, \quad (2)$$

where: M is the total mass of the structure, and EA is the total impact energy.

The purpose of the honeycomb structure is to reduce the hydraulic leg stress, and the optimization function of honeycomb structure can be constructed based on the stress of hydraulic leg:

$$\begin{cases} \min \{ \sigma(x) \} \\ s.t. x \in R^n \text{ and } x_L \leq x \leq x_U \end{cases}, \quad (3)$$

where: x_L and x_U are the left and right boundaries of the design variables, respectively. For the honeycomb structure $x = (D, L, p)$; D is cell size; L is cell thickness; p is cell height. The range of these three variables is designed according to the previous impact response law, $8 \text{ mm} \leq D \leq 10 \text{ mm}$, $18 \text{ mm} \leq L \leq 22 \text{ mm}$, $0.1 \text{ mm} \leq p \leq 1.3 \text{ mm}$, and Eq. (3) can be written as:

$$\begin{cases} \min \{ \sigma(x) \} \\ s.t. \quad 8 \text{ mm} \leq D \leq 10 \text{ mm} \\ \quad \quad 18 \text{ mm} \leq L \leq 22 \text{ mm} \\ \quad \quad 0.1 \text{ mm} \leq p \leq 0.3 \text{ mm} \end{cases}. \quad (4)$$

4.2. Orthogonal experimental design

Three factor and three level orthogonal test is used to study the impact resistance of honeycomb structures with different geometric parameters. The three factors chosen for the test are A , the cell size, B , the cell wall thickness, and C , the cell height. Three levels are selected for each factor, and the values of the design variables are filled into the orthogonal table, respectively. The specific scheme is shown in Table 5.

Table 5

Orthogonal test scheme, mm

Number	Cell size	Cell thickness	Cell height
1	1	1	1
2	1	2	2
3	1	3	3
4	2	1	3
5	2	2	1
6	2	3	2
7	3	1	2
8	3	2	3
9	3	3	1

4.3. Results and analysis

The roof displacement and hydraulic leg stress of different schemes are extracted using the range method, the range data is determined, and the optimal combination of each level factor within their respective index range is obtained, as shown in Tables 6 and 7.

Table 6

Orthogonal test and range under stress index

Test	Factor			Stress
	A	B	C	
1	1	1	1	1.617e+08
2	1	2	2	6.376e+07
3	1	3	3	6.549e+07
4	2	1	3	3.127e+07
5	2	2	1	3.041e+07
6	2	3	2	5.438e+07
7	3	1	2	3.476e+07
8	3	2	3	3.285e+07
9	3	3	1	3.845e+07
K1	2.909e+08	2.277e+08	2.305e+08	
K2	1.160e+08	1.270e+08	1.529e+08	
K3	1.061e+08	1.583e+08	1.296e+08	
K11	9.696e+07	7.590e+07	7.683e+07	
K22	3.866e+07	4.233e+07	5.096e+07	
K33	3.536e+07	5.276e+07	4.320e+07	
R	1.31e+07	2.536e+07	2.259e+07	
Weight of influencing factors				$B>C>A$

$K1$, $K2$, and $K3$ represents the index sum of each factor at the first, second, and third levels, respectively; $K11$, $K22$, and $K33$ represents the index average of each factor at the first, second, and third levels, respectively; R is the range

value of the evaluation index, and the larger the value, the greater the influence on the optimization target. As can be seen from Tables 6 and 7, cell thickness has the greatest impact on impact resistance, considering the hydraulic leg stress and roof displacement as the evaluation indexes, the optimal combination is $A_2B_2C_1$ and $A_3B_1C_1$, respectively.

Table 7

Orthogonal test and range under displacement index

Test	factor			Displacement
	A	B	C	
1	1	1	1	0.2699
2	1	2	2	0.4710
3	1	3	3	0.8470
4	2	1	3	0.2628
5	2	2	1	0.4490
6	2	3	2	0.5574
7	3	1	2	0.2259
8	3	2	3	0.3921
9	3	3	1	0.5869
K1	1.5879	0.7586	1.3058	
K2	1.2692	1.3121	1.2543	
K3	1.2049	1.9913	1.5019	
K11	0.5293	0.2528	0.4352	
K22	0.4230	0.4373	0.4181	
K33	0.4016	0.6637	0.5006	
R	0.1277	0.4109	0.0825	
Weight of influencing factors				B>A>C

Matrix analysis was used to further explore the optimal combination of different parameters. Create the target matrix M , assuming that the orthogonal test is 1 factor m level, the mean value of evaluation index of factor A_j at the j -th level is k_{ij} . If the evaluation index is larger and better, then $K_i = K_{ij}$ (Conversely, take the reciprocal):

$$M = \begin{bmatrix} K_{11} & 0 & 0 & \dots & 0 \\ K_{12} & 0 & 0 & \dots & 0 \\ \dots & \dots & \dots & \dots & \dots \\ K_{1m} & 0 & 0 & \dots & 0 \\ 0 & K_{21} & 0 & \dots & 0 \\ 0 & K_{22} & 0 & \dots & 0 \\ \dots & \dots & \dots & \dots & \dots \\ 0 & K_{2m} & 0 & \dots & 0 \\ \dots & \dots & \dots & \dots & \dots \\ 0 & 0 & 0 & \dots & K_{j1} \\ 0 & 0 & 0 & \dots & K_{j2} \\ \dots & \dots & \dots & \dots & \dots \\ 0 & 0 & 0 & \dots & K_{jm} \end{bmatrix},$$

$$T = \begin{bmatrix} T_1 & 0 & 0 & 0 \\ 0 & T_2 & 0 & 0 \\ \dots & \dots & \dots & \dots \\ 0 & 0 & 0 & T_l \end{bmatrix} \left(T_i = 1 / \sum_{j=1}^m K_{ij} \right), \quad (5)$$

Assume that the range of the A_i factor is s_i , set $S_i = s_i / \sum_{i=1}^l s_i$, establish the matrix S of the level layer and the weight matrix of evaluation index ω .

$$S = [S_1 \ S_2 \ \dots \ S_l]^T,$$

$$\omega = MTS = [\omega_1 \ \omega_2 \ \dots \ \omega_m], \quad (6)$$

where: $\omega_1 = K_{11}T_1S_1$, $K_{11}T_1 = K_{11} / \sum_{j=1}^m K_{1j}$ represent the proportion of the first level value of factor A_1 under the current evaluation index; $S_i = s_i / \sum_{i=1}^l s_i$ represent the range proportion of factor A_i under the current evaluation index; w_1 reflects the range and degree of influence of each factor under the current evaluation index. According to the above formula, the weight of each factor under the current index is calculated to determine the optimal combination.

The stress on the hydraulic leg is taken as the evaluation index, and the weight matrix is:

$$\omega_1 = M_1T_1S_1 = \begin{bmatrix} 0.3438 & 0 & 0 \\ 0.8620 & 0 & 0 \\ 0.9425 & 0 & 0 \\ 0 & 0.4391 & 0 \\ 0 & 0.7874 & 0 \\ 0 & 0.6317 & 0 \\ 0 & 0 & 0.4338 \\ 0 & 0 & 0.6540 \\ 0 & 0 & 0.7716 \end{bmatrix} \times \begin{bmatrix} 1 & 0 & 0 \\ 5.130 & 1 & 0 \\ 0 & 5.130 & 0 \\ 0 & 0 & 1 \\ 5.130 & 0 & 0 \end{bmatrix} \times \begin{bmatrix} 0.1310 \\ 0.6105 \\ 0.2536 \\ 0.6105 \\ 0.2259 \\ 0.6105 \end{bmatrix} = \begin{bmatrix} 0.0144 \\ 0.0360 \\ 0.0393 \\ 0.0357 \\ 0.0636 \\ 0.0511 \\ 0.0315 \\ 0.0470 \\ 0.0555 \end{bmatrix} \quad (7)$$

The roof displacement is taken as the evaluation index, and the weight matrix is:

$$\omega_2 = M_2T_2S_2 = \begin{bmatrix} 0.6298 & 0 & 0 \\ 0.7879 & 0 & 0 \\ 0.8299 & 0 & 0 \\ 0 & 1.3182 & 0 \\ 0 & 0.7621 & 0 \\ 0 & 0.5021 & 0 \\ 0 & 0 & 0.7658 \\ 0 & 0 & 0.7973 \\ 0 & 0 & 0.6658 \end{bmatrix} \times \begin{bmatrix} 1 & 0 & 0 \\ 4.062 & 1 & 0 \\ 0 & 4.062 & 0 \\ 0 & 0 & 1 \\ 4.062 & 0 & 0 \end{bmatrix} \times \begin{bmatrix} 0.1277 \\ 0.6211 \\ 0.4109 \\ 0.6211 \\ 0.0825 \\ 0.6211 \end{bmatrix} = \begin{bmatrix} 0.0319 \\ 0.0399 \\ 0.0420 \\ 0.2147 \\ 0.1241 \\ 0.0818 \\ 0.0250 \\ 0.0261 \\ 0.0218 \end{bmatrix} \quad (8)$$

The total weight matrix is obtained by taking the mean of the two indexes as the standard:

$$\omega = \frac{\omega_1 + \omega_2}{2} = \frac{1}{2} \times \left(\begin{bmatrix} 0.0144 \\ 0.0360 \\ 0.0393 \\ 0.0357 \\ 0.0636 \\ 0.0511 \\ 0.0315 \\ 0.0470 \\ 0.0555 \end{bmatrix} + \begin{bmatrix} 0.0319 \\ 0.0399 \\ 0.0420 \\ 0.2147 \\ 0.1241 \\ 0.0818 \\ 0.0250 \\ 0.0261 \\ 0.0218 \end{bmatrix} \right) = \begin{bmatrix} 0.0232 \\ 0.0380 \\ 0.0407 \\ 0.1252 \\ 0.0939 \\ 0.0665 \\ 0.0283 \\ 0.0366 \\ 0.0387 \end{bmatrix} = \begin{bmatrix} A_1 \\ A_2 \\ A_3 \\ B_1 \\ B_2 \\ B_3 \\ C_1 \\ C_2 \\ C_3 \end{bmatrix}. \quad (9)$$

According to the weight value, the importance of each factor under the current evaluation index can be obtained as $B > C > A$. (cell thickness > cell side > cell height), and A_3 , B_1 , and C_3 is the optimal combination.

5. Conclusions

To reduce the deleterious effects of rock burst on underground operation, a honeycomb anti-impact structure acting on the roof of the hydraulic support is proposed. The mechanical model of the hydraulic support was established, and the effect of geometric parameters on the impact resistance of the honeycomb structure was studied. The honeycomb structure was optimized by orthogonal test, and the following results were obtained:

1. With the increase in cell size, the maximum stress of the hydraulic leg decreases first and then increases, and the roof displacement gradually decreases. The increase in cell thickness leads to a gradual increase in the maximum stress of the hydraulic leg, and the roof displacement decreases first and then increases. When the honeycomb height increases, the maximum hydraulic pushing stress increases gradually, and the roof displacement decreases first and then increases.

2. When the hydraulic leg stress was used as the evaluation index, the cell thickness had the greatest influence on the impact resistance of the structure, followed by the cell height. When roof displacement is considered the evaluation index, the cell thickness has the greatest influence, followed by cell size. Combined with the two evaluation indexes, the order of influence of each factor was obtained by matrix analysis: cell thickness > cell size > cell height.

References

1. **Wang, X. B.; Tian, F.; Bai, X. Y.; Guo, X.** 2020. Numerical simulation of deformation and cracking process of rectangular roadway under different impact velocities, *Vibration and Shock* 33(14): 94-101 + 108.

- <https://doi.org/10.13465/j.cnki.jvs.2020.14.014>.
2. **Feng, Y. F.; Li, H. Y.; Du, L. L.; Li, Y. Q.** 2020. 70 years' experience, effect, situation analysis and prospect of coal mine safety production in China, *Journal of China Coal* 46-48 (05): 47-56. <https://doi.org/10.19880/j.cnki.ccm.2020.05.010>.
3. **Chen, Y. F.; Li, X. J.; Wu, H. B.** et al. 2021. Control status and development trend of rockburst mechanism and prevention in China, *Coal Science and Technology* 42(05): 70-75. <https://doi.org/10.19896/j.cnki.mtkj.2021.05.016>.
4. **Gao, M. S.; He, Y. L.; Xu, D.; Yu, X.** 2021. Principle and application of reduce and isolation technology in rock burst roadway, *Coal Science and Technology* 49(06): 53-60. <https://doi.org/10.13199/j.cnki.cst.2021.06.006>.
5. **Hou, Y.** 2019. Optimizing the key structures of statically indeterminate hydraulic support in fully-mechanized caving face, *Coal Mine Modernization* 05: 114-117. <https://doi.org/10.13606/j.cnki.37-1205/td.2019.05.037>.
6. **Pan, Y. S.; Xiao, Y. H.; Li, G. Z.** 2020. Roadway hydraulic support for rockburst prevention in coal mine and its application, *Journal of China Coal Society* 45(01): 90-99. <https://doi.org/10.13225/j.cnki.jccs.YG19.1762>.
7. **Hao, Z. Y.; Liu, Y. Q.; Pan, Y. S.** 2018. Experimental study on filling material of mining buffer energy absorption device, *Journal of Mining and Safety Engineering* 35 (3): 620-628. <https://doi.org/10.13545/j.cnki.jmse.2018.03.024>.
8. **Ma, X.; Pan, Y. S.; Zhang, J. Z.; Xiao, Y. H.** 2018. Design and performance research on core energy absorption component of anti-impact support, *Journal of China Coal Society* (4): 1171-1178. <https://doi.org/10.13225/j.cnki.jccs.2017.0693>.
9. **Tang, Z.; Pan, Y. S.; Zhu, X. J.; Cui, N. X.** 2017. Design of constant resistance giving way and anti-impact device of mining column and its characteristic analysis, *Journal of Chongqing University* 40(06): 54-59. <https://doi.org/10.11835/j.issn.1000-582X.2017.06.007>.
10. **Tang, Z.; Pan, Y. S.; Zhu, X. J.; Cui, N. X.** 2016. Design and study of self-moving energy absorption and anti-impact roadway advanced support, *Journal of China Coal Society* 9 (4): 1032-1037. <https://doi.org/10.13225/j.cnki.jccs.2015.1159>.
11. **Xu, S.; Beynon, J. H.; Ruan, D.; Yu, T. X.** 2012. Strength enhancement of aluminium honeycombs caused by entrapped air under dynamic out-of-plane compression, *International Journal of Impact Engineering* 47:1-13. <https://doi.org/10.1016/j.ijimpeng.2012.02.008>.
12. **Zhang, X.; Zhang, H.; Wen, Z. Z.** 2014. Experimental and numerical studies on the crush resistance of aluminium honeycombs with various cell configurations, *International Journal of Impact Engineering* 66: 48-59. <https://doi.org/10.1016/j.ijimpeng.2013.12.009>.
13. **Hou, B.; Pattofatto, S.; Li, Y. L.; Zhao, H.** 2011. Impact behavior of honeycombs under combined shear-compression. Part II: Analysis, *International Journal of Solids & Structures* 48(5): 698-705. <https://doi.org/10.1016/j.ijsolstr.2010.11.004>.
14. **Li, Z. Q.; Xi, C. Q.; Lin, J.**; et al. 2014. Effect of loading rate on the compressive properties of open-cell metal

foams, *Materials Science & Engineering A*(592) : 221-229.

<https://doi.org/10.1016/j.msea.2013.11.011>.

15. **Yungwirth, C. J.; Wadley, H. N. G.; O'Connor, J. H.** et al. 2008. Impact response of sandwich plates with a pyramidal lattice core, *International Journal of Impact Engineering* 35(8): 920-936.
<https://doi.org/10.1016/j.ijimpeng.2007.07.001>.

Q. Zhang, B. Li, R. Zhang

OPTIMIZATION OF ANTI-IMPACT ENERGY ABSORPTION STRUCTURE OF HYDRAULIC SUPPORT

S u m m a r y

Rock bursts are a frequent occurrence in deep coal mining, and reducing the risk of rock bursts is necessary for

the safe and efficient mining of coal. As honeycomb structures have good impact resistance, the design suggests that a honeycomb structure is adopted in the roof. A mechanical model of the hydraulic support is established, and the influence of geometric parameters on the impact resistance of the honeycomb structure is studied. Finally, the orthogonal test method was used to analyze the influence and weight of the geometric parameters on the anti-impact performance of the honeycomb structure with hydraulic leg stress and roof displacement as the evaluation indexes. This paper provides a new design idea for the research and development of an impact resistance hydraulic support in the underground coal mine, which is significant in ensuring coal mine safety.

Keywords: rock burst, cellular, orthogonal test, optimize.

Received March 08, 2022

Accepted August 24, 2022



This article is an Open Access article distributed under the terms and conditions of the Creative Commons Attribution 4.0 (CC BY 4.0) License (<http://creativecommons.org/licenses/by/4.0/>).